4622 *Macromolecules* **2009**, *42*, 4622–4631
DOI: 10.1021/ma802834x

Macromolecules
ARTICLE

A General Method for the Synthesis and Isolation of Well-Defined Core Cross-Linked Multistar Assemblies: A Route toward Enhanced pH-Responsive Polymers

Jing Fung Tan, Anton Blencowe, Tor Kit Goh, Irving Ted M. Dela Cruz, and Greg G. Qiao*

Polymer Science Group, Department of Chemical & Biomolecular Engineering, The University of Melbourne, Melbourne, Victoria 3010, Australia

Received December 21, 2008; Revised Manuscript Received April 6, 2009

ABSTRACT: A general method for the synthesis of well-defined multistar assemblies (in which the stars contain cross-linked cores) involving the atom transfer radical polymerization (ATRP) of macroinitiators (MIs) and cross-linker with the use of telechelic macroinitiators (TMIs) as the connecting blocks is described. Isolation of each type of multistar assembly with a high degree of specificity was achieved via a simple fractional precipitation process. Selective degradation of the PMMA-based and P^{t}BMA-based multistar assemblies into their individual star units via cleavage of the disulfide group within the connecting blocks confirmed the synthesis of well-defined, low-polydispersity PMMA-based tristar and dumbbell polymers and P^{t}BMA-based tetrastar, tristar, and dumbbell polymers. Hydrolysis of the P^{t}BMA-based assemblies afforded amphiphilic poly(methacrylic acid) (PMAA) multistar assemblies and dumbbell polymers with enhanced pH responsiveness over their single star analogues, with changes in d_h of 42% and 30%, respectively (this is in comparison to 22% for discrete PMAA CCS polymers). Furthermore, the first reported native-state images of these PMAA-based multistar assemblies and CCS polymers in solution obtained using cryogenic transmission electron microscopy (cryo-TEM) are presented, revealing the different conformations of the various multistar assemblies.

Introduction

The behavior of materials in response to changes in their external environment has been extensively exploited in a variety of applications, including controlled drug release from nanocapsules and targeted molecule detection by biosensors.[1,2] However, the responsiveness of the materials to stimuli could be encumbered by their inherent properties, thus limiting the process efficacy. With nanotechnology being recognized as one of the main areas of research in targeted detection and delivery,[3] the search for novel nanoscale materials with a more dynamic response to specific stimuli has been the subject of intense research.

Core cross-linked star (CCS) polymers are architecturally unique macromolecules with linear polymeric arms radiating from a central cross-linked core. They are typically synthesized via living polymerization methods such as anionic[4] and controlled radical techniques.[5] A recent addition is the application of ring-opening polymerization in the synthesis of CCS polymers with different degrees of degradability.[6,7] Researchers have exploited these polymers for the unique nanoenvironments created by the shielding of their central cross-linked cores from the external environment by a corona of arms, with these polymers being utilized in a variety of applications including acid−base-catalyzed cascade[8] and ruthenium-catalyzed reactions.[9]

It was envisioned that the synthesis of well-defined multistar analogues of CCS polymers would provide advanced materials with additional features important for a wide variety of nanotechnologies. For example, most payload delivery nanocapsules induce either reversible or irreversible conformational changes in response to external stimuli such as temperature or pH to elicit the release of their payloads (with the magnitude of the changes being dependent on their structure and composition).[1] Enhanced-response payload delivery vehicles could be achieved by the synthesis of amphiphilic pH-sensitive multistar assemblies, since the increased number of entities within each assembly amplifies any response to pH changes, while the amphiphilicity of the polymer imparts self-assembling properties.[10−14]

To date, the preparation and isolation of these complex macromolecules has been difficult due to the formation of uncontrolled insoluble networks similar to those produced during reaction of end-functionalized star polymers with difunctional cross-linkers[15,16] or during the cross-linking of macromonomers with multifunctional cross-linkers.[17] Methods to circumvent these problems, such as high dilution synthesis, would inevitably require copious amounts of solvents in order to obtain significant amounts of product. As a result, such synthetic procedures are generally unattractive.

Herein, a general and facile method for synthesizing multistar assemblies (containing cross-linked cores) in high yield via ATRP is reported. The number of CCS stars within each assembly can be tailored by adjusting the M_w and molar ratio of the connecting blocks (referred to as telechelic macroinitiators (TMIs)) used during the synthesis. These polymers were also separated into each type of well-defined multistar assembly (tetrastar, tristar, and dumbbell polymers) via a simple fractionation process. Cleavage of the disulfide bridge within the TMIs allows selective degradation of these assemblies into their constituent star components and offers conclusive evidence for the synthesis of these well-defined multistar assemblies. In addition, seminal native-state images of the amphiphilic PMAA multistar assemblies in solution via cryo-TEM analysis show them in their tetrastar, tristar, and dumbbell conformations. These amphiphilic multistar assemblies possess an

*To whom correspondence should be addressed.

 Published on Web 06/05/2009

Scheme 1. Synthesis and Cleavage of PMMA-Based Dumbbell Polymers and Multistar Assemblies

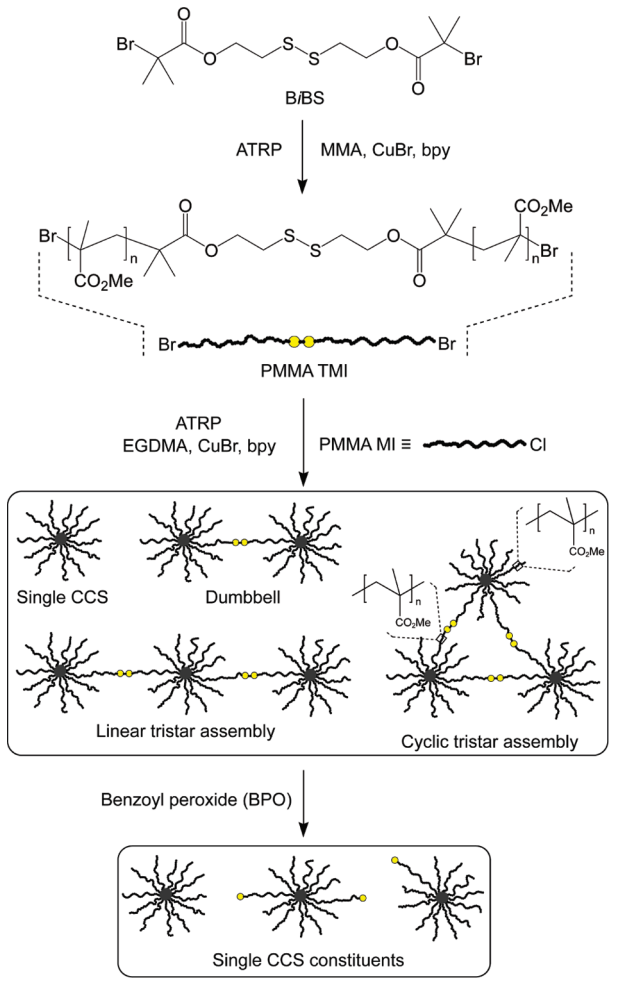

enhanced pHs-responsiveness over their CCS polymer counterparts, illustrating the potential of these polymers to be further developed for a wide range of nanostructured materials.

Results and Discussion

The synthesis of multistar assemblies was achieved by ATRP of living poly(methyl methacrylate) (PMMA) macroinitiators (MIs) in the presence of a cross-linker (ethylene glycol dimethacrylate (EGDMA)) and a cleavable disulfide telechelic macroinitiator (TMI). EGDMA serves as a cross-linking agent during the star polymer formation, which results in a star-shaped macromolecule consisting of a corona of linear PMMA arms emanating from a central cross-linked poly(EGDMA) core.[5,6] The addition of a TMI into the reaction mixture results in the in situ formation of core cross-linked multistar assemblies as the terminal groups of the TMIs become incorporated into the architecture of different stars during the cross-linking process with EGDMA, thus linking them together (Scheme 1). This also allows a greater degree of control in the formation of these multistar assemblies in comparison to postpolymerization attachment of end-functionalized CCS stars to connectors with a complementary functionality.

The incorporation of a disulfide bridge within the TMIs allowed selective cleavage of the resulting multistar assemblies into their constituent single star components, thus providing evidence for their assigned structures, as the magnitude of the reduction in M_w upon cleavage would provide information pertaining to the number of CCS polymers within each assembly (Scheme 1).

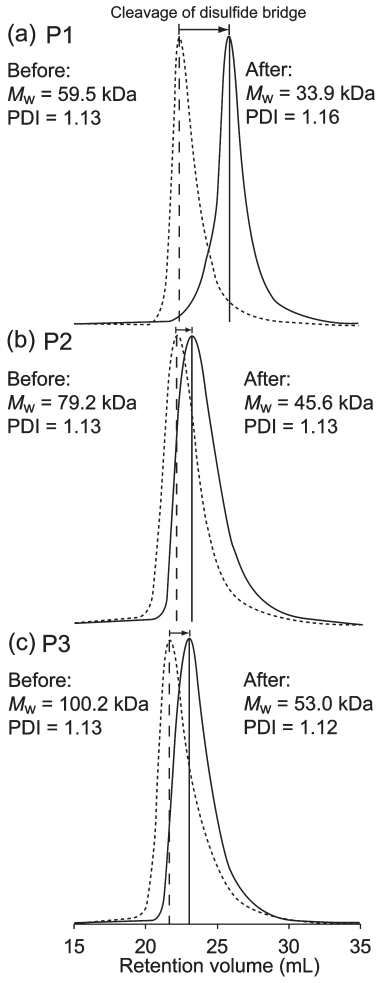

Figure 1. GPC RI traces of (a) **P1**, (b) **P2**, and (c) **P3** before (- - -) and after (—) cleavage with BPO. Polymer M_ws as determined by GPC-MALLS were observed to reduce by approximately half.

Preparation of PMMA Telechelic Macroinitiators (TMIs). The difunctional ATRP initiator, bis[2-(2-bromoisobutyryloxy)ethyl] disulfide (B*i*BS) (Supporting Information section S1), was employed to synthesize a series of PMMA TMIs of different M_w (60, 80, and 100 kDa) via ATRP. All of the TMIs displayed characteristic "living" behavior in chain extension experiments (Supporting Information section S2). Treatment of the TMIs with benzoyl peroxide (BPO) yielded cleaved TMIs with half the original M_w, while maintaining a low PDI (PDI < 1.16) (Figure 1).[18,19] These results indicate that the initiating sites of the initiator, B*i*BS, have equal reactivity and that the resulting TMIs **P1**−**3** (60, 80, and 100 kDa, respectively) contain a centrally located disulfide bridge. Cleavage of the chain-extended TMIs also resulted in a halving of the original M_w, indicating that the "living" ends of the TMIs are almost completely conserved.

Synthesis of PMMA-Based Multistar Assemblies P4−**12.** The PMMA TMIs were employed to synthesize core cross-linked multistar assemblies and dumbbell polymers via ATRP with PMMA MI and EGDMA. The typical synthetic and fractionation processes, as followed by GPC and DLS, are shown in Figure 2. The PMMA MI and TMI **P1** were polymerized with EGDMA to yield a crude reaction product **P4** (containing multistar assemblies and CCS polymers). Each of the different types of multistar assemblies present in **P4** was then isolated via fractional precipitation to obtain four separate fractions, **P4a**−**d** (Table 1).

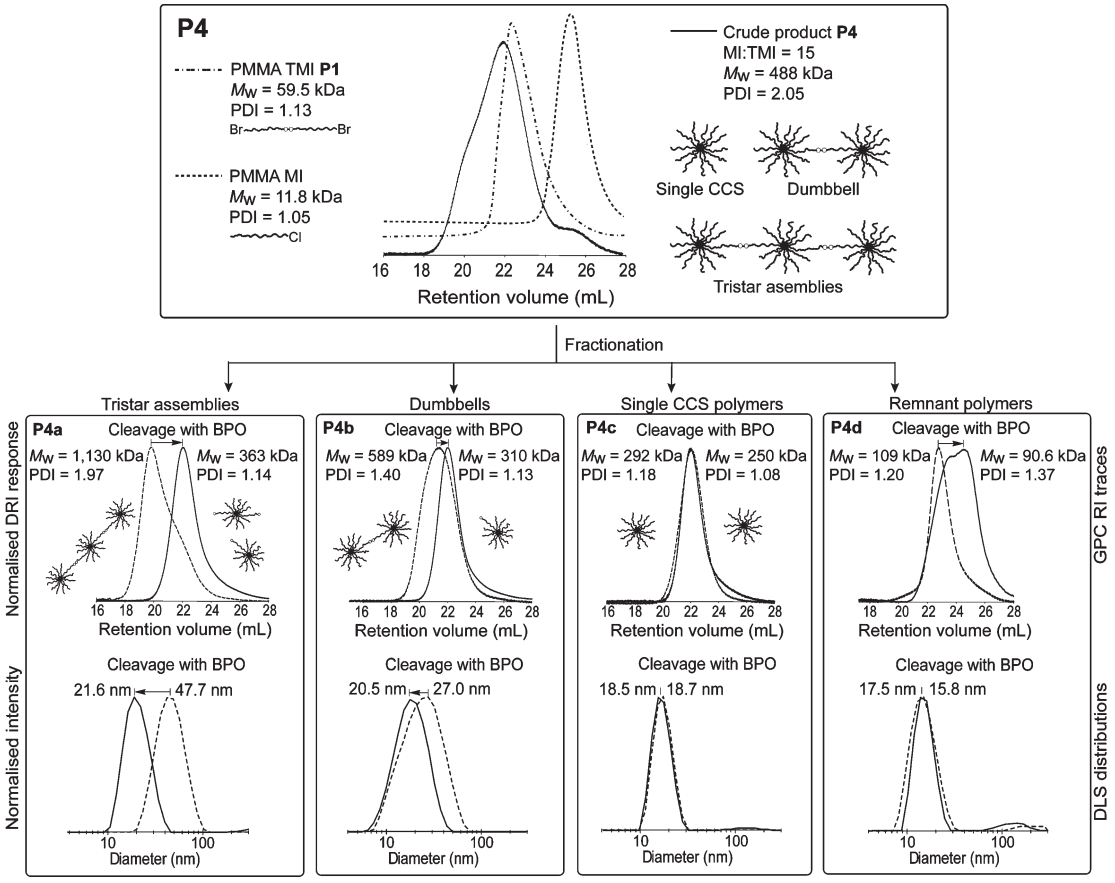

Figure 2. GPC RI trace of **P4** synthesized using TMI **P1** (MI:TMI = 15) and PMMA MI and GPC and DLS traces of **P4** fractionation to afford polymers **P4a−d** and their subsequent cleavage with BPO. Properties of **P4** and its respective fractions are listed in Table 1.[20]

These fractions were subsequently degraded into their constituent single CCS polymer components by treatment with BPO (Figure 2).

The corresponding reduction in M_w of the polymer fractions upon cleavage (**P4a**: by $^1/_3$; **P4b**: by $^1/_2$; and **P4c**: unchanged) confirmed the successful synthesis and isolation of tristar assemblies, dumbbells, and single CCS polymers (**P4a−c**, respectively) (Table 1). Interestingly, cleavage of **P4d** resulted in the formation of a bimodal RI trace (Figure 2), indicating that this fraction contained TMIs that had not reacted to form assemblies or had only partially reacted to form relatively low molecular weight species. The CCS polymers obtained after BPO cleavage of **P4a−c** possessed M_ws of 363, 310, and 250 kDa, respectively, which corresponded well with the M_w of the discrete CCS polymer **P13** (M_w = 254 kDa; synthesized using an identical formulation in the absence of TMIs) (Table 1), if the additional mass of the cleaved TMI segments are taken into consideration. Therefore, the addition of TMI does not significantly affect the dynamics of the CCS polymer formation reaction, with an optimum of ca. 18−20 arms per CCS polymer persisting regardless of whether the star is singular or part of a larger assembly.

The GPC results were also supported by DLS analysis. The reduction in d_h of **P4a** and **P4b** from 47.7 and 27.0 nm to 21.6 and 21.5 nm, respectively, and the constant d_h of **P4c** (18.7 nm) provide further evidence for the successful cleavage of the assemblies into their constituent stars after reaction with BPO (Figure 2 and Table 1). The similar d_h values and low polydispersities (PDI < 1.17) of the cleaved products as determined by DLS and GPC, respectively, indicate that the CCS polymers from which the assemblies were composed are nearly identical.

By systematic variation of the MI:TMI ratio[21] (15:1, 25:1, and 35:1) and TMI M_w (60 (**P1**), 80 (**P2**), and 100 kDa (**P3**)), a series of polymers (**P4−12**) were prepared (**P4−6**: TMI M_w = 60 kDa; **P7−9**: TMI M_w = 80 kDa; and **P10−12**: TMI M_w = 100 kDa). This enabled the effect of TMI M_w and concentration on the formation of multistar assemblies to be studied. In an identical fashion to **P4**, the crude product mixtures **P5−12** were fractionally precipitated into their constituent polymeric species and characterized via GPC-MALLS and DLS (refer to Table 1 for detailed characterization of **P5−7**, **P10**, and their fractionated products; refer to Supporting Information section S3 for detailed characterization of **P8−9**, **P11−12**, and their fractionated products). From the BPO-mediated disulfide cleavage of the fractionated polymers, it was confirmed that the crude polymer products **P4−6** synthesized using TMI **P1** comprised of tristar assemblies, dumbbells, and CCS polymers, while **P7−12** prepared using TMIs **P2** and **P3** consisted of only dumbbell and CCS polymers.[22] The similar d_h values and low polydispersities (PDI < 1.17) of the cleaved products as determined by DLS and GPC, respectively, indicate the uniformity of the CCS polymers from which the assemblies were composed.

The effects of varying MI:TMI molar ratio (constant TMI **P1** M_w = 60 kDa) and TMI M_w (constant MI:TMI = 15) on the resulting multistar assemblies' M_w, d_h, and yield are summarized in Figure 3. At a constant TMI molecular weight, an increase in the MI:TMI ratio had a negligible effect upon the M_w and d_h values of the resulting tristar assemblies, dumbbells, and CCS polymers (Figure 3a), whereas the yield of tristar assemblies and dumbbells decreased as the MI:TMI ratio was increased (Figure 3b).

Table 1. Detailed Characterization of PMMA-Based Multistar Reaction Mixtures P4−7, P10, and Their Fractionated Products before and after Cleavage with Benzoyl Peroxide and CCS Polymer P13

				before cleavage					after cleavage			
polymer	polymer fraction	$M_{w(TMI)}$[b] (kDa)	MI:TMI	$M_{w(product)}$[b] (kDa)	PDI[b]	d_h[c] (nm)	f[d]	yield (%)	$M_{w(product)}$[b] (kDa)	PDI[b]	d_h[c] (nm)	f[d]
P4	unfractionated	59.5	15	488	2.05			74.2[e]				
P4a	tristar			1130	1.97	47.7	77	25.5[f]	363	1.14	21.6	25
P4b	dumbbell			589	1.40	27.0	40	19.6[f]	310	1.13	20.5	21
P4c	single star			292	1.18	18.7	20	40.4[f]	250	1.08	18.5	17
P4d	remnant			109	1.20	15.8		14.5[f]	90.6	1.37	17.5	
P5	unfractionated	59.5	25	304	1.15			72.4[e]				
P5a	tristar			1120	1.25	45.4	76	8.5[f]	360	1.06	19.6	24
P5b	dumbbell			635	1.14	28.6	43	25.3[f]	297	1.06	17.8	20
P5c	single star			331	1.06	19.8	22	49.4[f]	279	1.04	18.5	19
P5d	remnant			224	1.04	16.3		16.8[f]	204	1.05	16.1	
P6	unfractionated	59.5	35	268	1.10			78.8[e]				
P6a	tristar			984	1.10	33.5	67	1.4[f]	349	1.07	17.4	24
P6b	dumbbell			616	1.06	23.1	42	9.5[f]	309	1.05	18.0	21
P6c	single star			283	1.06	17.7	19	69.9[f]	254	1.05	16.7	17
P6d	remnant			92.6	1.06	13.7		19.2[f]	88.2	1.12	13.2	
P7	unfractionated	79.2	15	340	1.55			87.9[e]				
P7a	dumbbell			773	1.11	30.2	52	23.6[f]	433	1.16	22.8	29
P7b	single star			365	1.05	19.3	25	51.8[f]	309	1.08	18.5	21
P7c	remnant			266	1.03	16.1		24.6[f]	192	1.17	15.9	
P10	unfractionated	100.2	15	452	1.41			81.1[e]				
P10a	dumbbell			531	1.29	27.3	36	63.5[f]	315	1.10	23.1	21
P10b	single star			307	1.14	22.5	21	28.9[f]	250	1.09	22.2	17
P10c	remnant			111	1.05	14.0		7.6[f]	96.4	1.12	13.6	
P13[a]				254	1.13		17	64.0[g]				

[a] Discrete CCS polymer prepared in the absence of TMI. [b] Determined by GPC-MALLS (dn/dc = 0.086 in THF). [c] Determined by DLS. [d] Arm number of the respective polymers.[23] [e] Determined gravimetrically. [f] Determination based upon mass recovery relative to unfractionated polymeric mixture being equal to 100%. [g] Yield of CCS polymer after fractional precipitation and isolation.

This trend is attributed to the different degree of MI and TMI incorporation into each macromolecule with varying MI:TMI ratio (Supporting Information section S4). When the TMI M_w was increased (> 60 kDa) at a constant MI:TMI ratio, the formation of tristar assemblies was not observed (Figure 3c), and interestingly, the yield of dumbbell polymers was found to increase (Figure 3b).

Synthesis of Poly(*tert*-butyl methacrylate) (P^{t}BMA)-Based Multistar Assemblies P14−16. To demonstrate the versatility of the synthetic approach, compositionally variable CCS polymer assemblies consisting of P^{t}BMA arms and cleavable PMMA connectors derived from the TMIs **P1−3** were prepared. The synthesis of these compositionally diverse macromolecules enables them to have hybrid chemical and physical properties derived from both polymeric components and allows postpolymerization modification of these polymers into amphiphilic pH-responsive multistar assemblies. The selection of different components for the arms and connectors also provides characterization advantages as it allows the determination of the relative ratios of MI and TMI components incorporated into the assemblies, which, along with GPC data, were features that were absent in the study of dumbbell-like polymers conducted by He et al.[24] Furthermore, as a result of the cleavable connectors, it has been possible to conclusively demonstrate that the assemblies and dumbbells are comprised of multiple well-defined CCS polymers, as opposed to being elongated or "wormlike" CCS polymers with fused cores. It has also been demonstrated that anisotropic multistar assemblies can be readily isolated without the need for lengthy dialysis procedures.

P^{t}BMA MI (M_w = 11.8 kDa, PDI = 1.14) and a MI:TMI ratio of 15:1 was used to synthesize P^{t}BMA-based assemblies as this ratio had previously provided the highest yield of PMMA-based multistar assemblies. In contrast to the crude PMMA-based polymeric mixtures **P4−12**, the M_ws of P^{t}BMA-based polymeric products **P14−16** were found to increase along with TMI M_w (Table 2). For comparative purposes, a discrete P^{t}BMA CCS polymer **P17** was also prepared using identical conditions, but in the absence of TMIs.

As before, fractionation and cleavage of the polymeric mixtures **P14−16** were carried out and investigated by GPC and DLS analyses. The M_w and d_h trends observed for the fractionated polymers are graphically summarized in Figure 4 with the detailed characterization of the polymers provided in Supporting Information section S5.

The results of the cleavage reactions conducted on the fractionated polymers indicated the presence of multistar assemblies (tetra- and tristar assemblies) in the crude polymer mixtures **P14−16**, in addition to dumbbell and CCS polymers. (GPC and DLS traces illustrating the reduction in M_w and d_h, respectively, of the fractionated polymers **P14a−c** after cleavage of the disulfide bonds are provided in Supporting Information sections S6 and S7.)

Calculations based upon integration of resonances in the ^{1}H NMR spectrum of **P14** (Figure 5) enabled the determination of the ratio of MMA to ^{t}BMA monomer units (1.0:1.0), which in turn provided an estimate of ca. 4 PMMA TMIs incorporated within each star (Supporting Information section S8). This indicates that the TMIs are not only found connecting individual star entities together but can also be tethered to single stars in a looped or dangled configuration.

Synthesis of pH-Responsive PMAA-Based Multistar Assemblies P18. The P^{t}BMA-based multistar product **P14** and CCS polymer **P17** were converted to poly(methacrylic acid) (PMAA)-based multistar assemblies **P18** and CCS polymer **P19**, respectively, via the acid hydrolysis of the *tert*-butyl ester groups present in the polymers. ^{1}H NMR spectroscopic

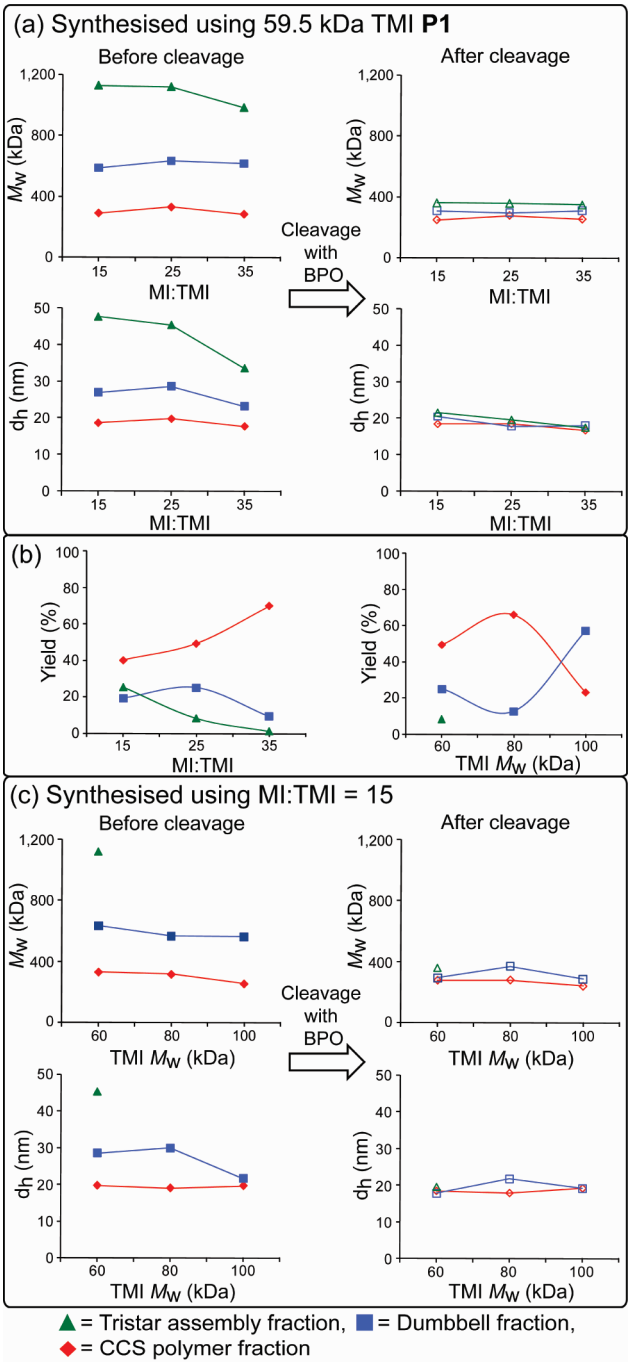

Figure 3. (a) Effect of varying MI:TMI molar ratio (constant TMI **P1** M_w = 60 kDa) on the M_w and d_h of tristar assemblies, dumbbells, and single CCS polymers before and after cleavage with BPO. (b) Effect of varying MI:TMI molar ratio (constant TMI **P1** M_w = 60 kDa) and TMI M_w (constant MI:TMI = 15) on the yield of tristar assemblies, dumbbells, and single CCS polymers. (c) Effect of TMI M_w (constant MI:TMI = 15) on the M_w and d_h of tristar assemblies, dumbbells, and single CCS polymers before and after cleavage with BPO. The error limits for the M_w and d_h values are ±5% and ±4%, respectively.

analysis of the PMAA-based multistar product **P18** and its precursors are presented in Figure 5 (^{13}C NMR spectra of **P18** and its precursors are provided in Supporting Information section S9). The successful trifluoroacetic acid (TFA)-mediated hydrolysis of the *tert*-butyl ester groups in **P14** was indicated by the disappearance of the *tert*-butyl proton resonances at ca. δ_H 1.4 ppm (Figure 5c, resonance **a**) and the appearance of a resonance at ca. δ_H 12.3 ppm (Figure 5d, resonance **d**) corresponding to the acid protons of **P18**.

Table 2. Characterization of P^{t}BMA-Based Polymer Mixtures P14−16 and CCS Polymer P17

polymer	$M_{w(TMI)}$[b] (kDa)	$M_{w(product)}$[b] (kDa)	PDI[b]	yield[c] (%)
P14	59.5	790	1.56	51.3
P15	79.2	808	2.05	42.5
P16	100.2	1130	1.66	43.4
P17[a]		487	1.39	30.0[d]

[a] Discrete CCS polymer prepared in the absence of TMI (f = 33). [b] Determined by GPC-MALLS (dn/dc = 0.090 in THF). [c] Determined gravimetrically. [d] Yield of CCS polymer after fractional precipitation and isolation.

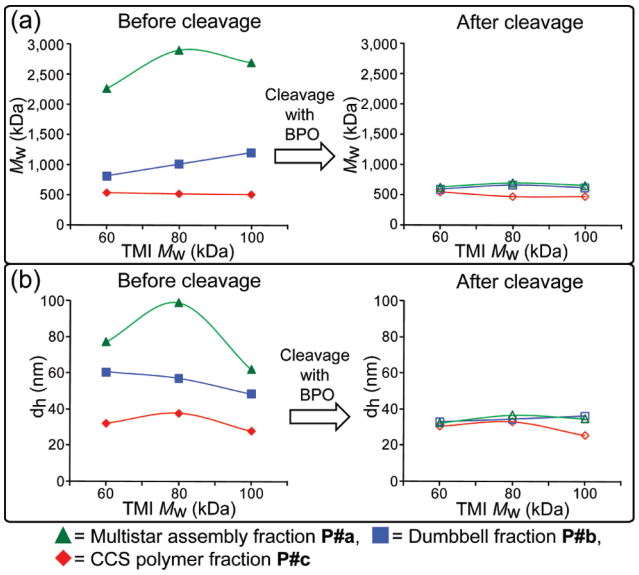

Figure 4. Graphical summaries of (a) M_w and (b) d_h vs TMI M_w for fractions **P#a−c** of **P14−16** before and after cleavage with BPO, illustrating the convergence of the M_ws and d_h to dimensions consistent with single CCS polymers. The error limits for the M_w and d_h values are ±6% and ±3%, respectively.

The reduction in M_w from 790 kDa (**P14**) to 651 kDa (**P18**) (as determined by GPC) corresponded very closely to the theoretical M_w (650 kDa), indicating almost complete hydrolysis of the *tert*-butyl ester groups (Supporting Information section S10). The efficiency of the hydrolysis reaction is also comparable with the acid hydrolysis of the P^{t}BMA CCS polymer **P17** (Supporting Information section S11).

Visual observation of CCS polymers using direct imaging methods have proved difficult despite the large amount of work published on the subject. To date, direct imaging of CCS polymer was mostly obtained using atomic force microscopy and transmission electron microscopy on substrates or in solid matrices;[9,25] this, inevitably, distorts the natural conformation of the star polymers due to the sample preparation. Native-state images of star-shaped polymers obtained via cryo-TEM have also been limited so far, with none reported for stars with cross-linked cores.[26] As such, direct visualization of CCS polymers in their native state is highly desirable for understanding their natural conformation and size.

The solubility of the synthesized amphiphilic PMAA-based multistar assemblies in aqueous solution enabled cryo-TEM of these macromolecular architectures in their solvated state to be conducted as the rapid freezing of the sample in vitreous ice instantly captures the polymer in its natural conformation. In order to ensure that the images obtained are truly of individual multistar assemblies and not of self-assembled multimacromolecular structures, cryo-TEM was carried out below the aggregation concentration

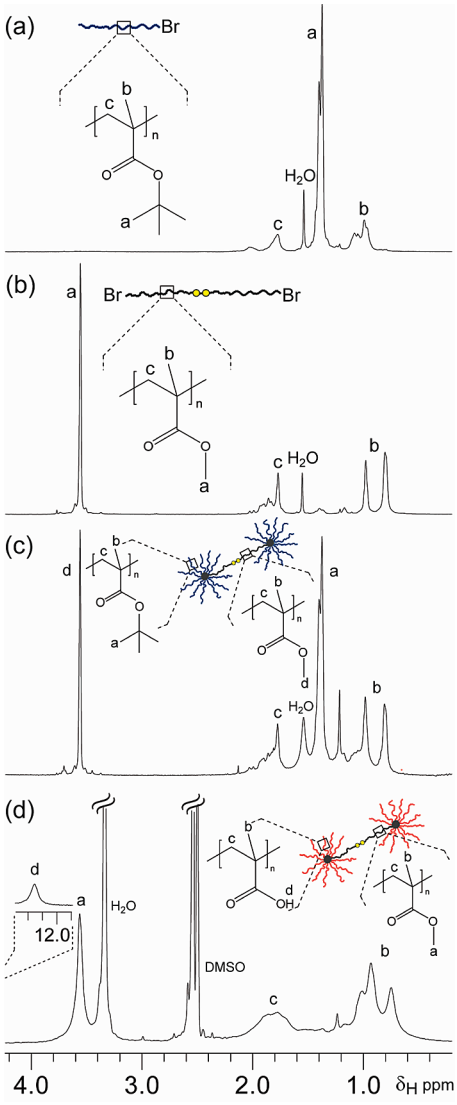

Figure 5. ^{1}H NMR spectra of (a) P^{t}BMA MI ($CDCl_3$), (b) PMMA TMI **P1** ($CDCl_3$), (c) P^{t}BMA-based **P14** ($CDCl_3$), and (d) PMAA-based **P18** (d_6-DMSO).

of the polymers (as determined by DLS). This also reduces the probability that images captured are a result of chain entanglement between CCS polymers, which may give the appearance of multistar assemblies or dumbbell polymers.

Cryo-TEM images of **P18** showed the presence of multistar assemblies (tetrastar and tristar assemblies), in addition to dumbbell and CCS polymers (Figure 6).[27] The difference in size between the constituent star components of the dumbbells is believed to result from the angular orientation of the macromolecules toward the camera. For comparative purposes, the discrete PMAA CCS polymer **P19** was analyzed using identical conditions. A histogram of 414 **P19** CCS polymers (Supporting Information section S12) indicated that the majority of the polymers had a diameter of 32 nm, which correlates closely to the value obtained via DLS (37.3 nm). This value also agrees well with the dimensions of the individual star components obtained from cleavage of the multistar assemblies.

pH-Responsiveness of PMAA-Based Multistar Assemblies P18. Given the pH-responsive nature of PMAA, amphiphilic assemblies such as **P18** could have applications in biological systems where water is a common solvating medium. The pK_a values of the PMAA-based multistar product **P18** and

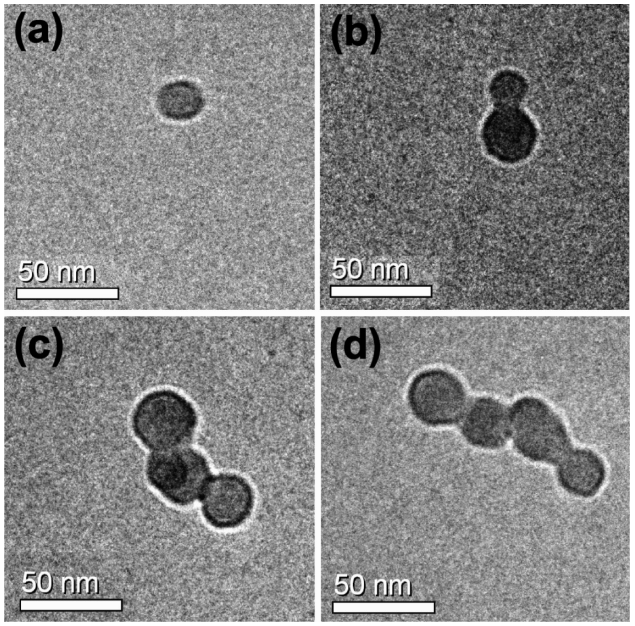

Figure 6. Cryo-TEM images of PMAA-based (a) CCS polymer **P19**, (b) **P18** dumbbell polymer, (c) **P18** tristar assembly, and (d) **P18** tetrastar assembly.

CCS polymer **P19** were calculated by pH titration experiments of aqueous polymer solutions at different degrees of ionization (Supporting Information section S13). The pK_a value of the CCS polymer **P19** was determined to be 6.9, which is in agreement with published values.[14] The larger pK_a value of 7.9 determined for the multistar product **P18** is likely due to the confined architecture of the polymer. The resultant increase in osmotic pressure causes a partial reversal of ionization which reduces the number of charged ions within the assembly. As a result, a higher pH is needed to achieve an activity coefficient (α) of 0.5.[28]

To demonstrate the pH responsiveness of these polymers, the relationship between pH and d_h was investigated via DLS analysis by reducing the pH of the solvating medium from an initial pH of 11.9. The d_h distributions measured by DLS of the PMAA-based multistar assembly product **P18** and CCS polymer **P19** at selected pH values are presented in parts a and b of Figure 7, respectively. Given that the multistar assembly **P18** was not fractionated into its constituent architectures, the multimodal peak distribution observed in the DLS traces clearly demonstrates the presence of multistar assemblies, dumbbells, and CCS polymers.

It was discovered that a reversible change in d_h could be induced by a change in medium pH. A reduction in d_h of the multistar assembly **P18** was observed upon decreasing the medium pH from 11.9 to 4.1, and aggregation of the polymers occurred with further reductions in pH (Figure 7a). Similar trends were observed for the CCS polymer **P19** upon a reduction in pH from 11.8 to 5.5, with a further decrease in pH resulted in aggregation of the polymers as indicated by an increase in d_h to 770 nm (Figure 7b).

Two different conformational behaviors were observed either side of the aggregation pHs[29] of 4.1 for the multistar product **P18** and 5.5 for the pure CCS polymer **P19**. Above these values, an increase in pH resulted in a corresponding increase in the d_h values, which results from an increased charge repulsion between the arms of the polymers, causing them to adopt an extended conformation. As the degree of ionization decreased with pH, the reduction in electrostatic repulsion between the arms resulted in the polymers

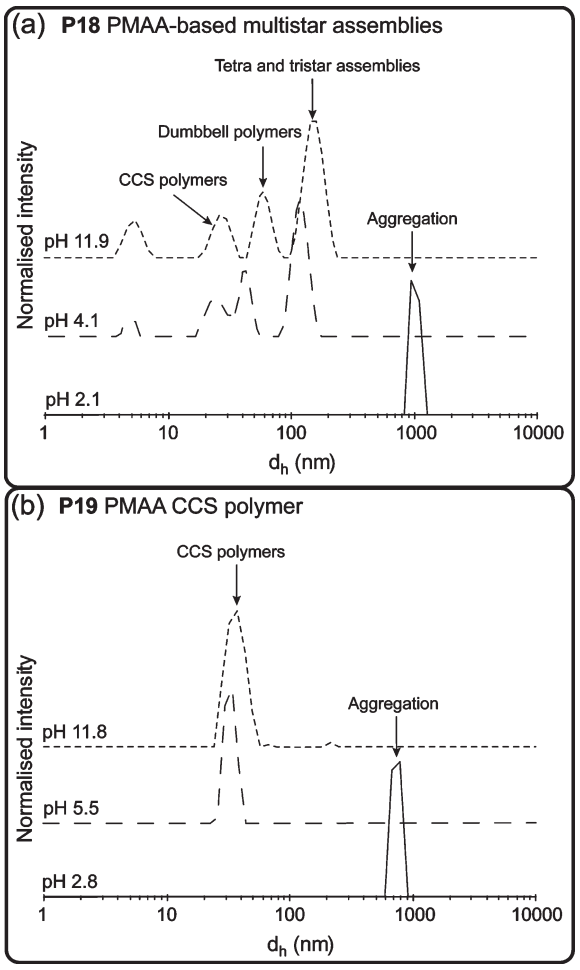

Figure 7. DLS traces of the (a) PMAA-based multistar assembly **P18** and (b) PMAA CCS polymer **P19**.

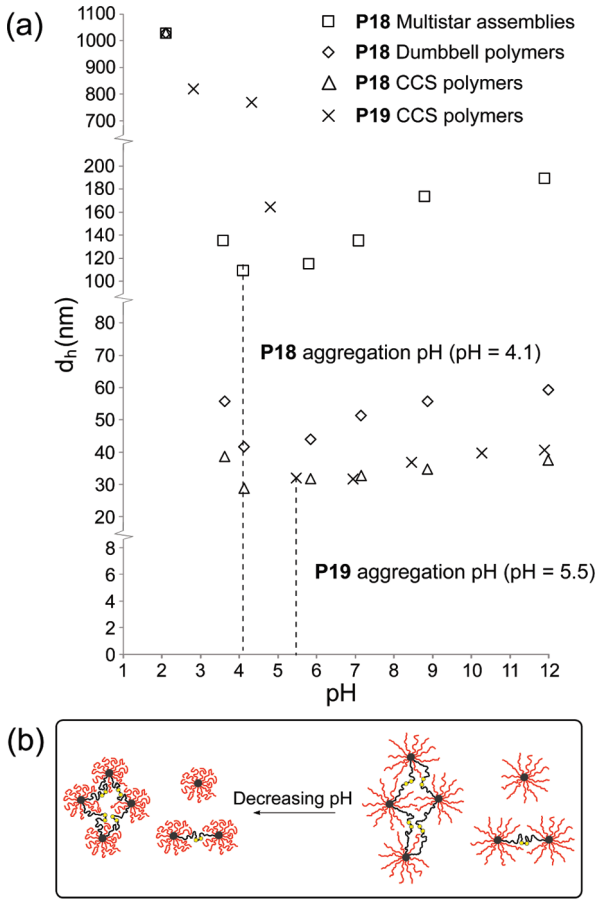

Figure 8. (a) Relationship between d_h and pH of PMAA-based CCS polymers **P19** and **P18** multistar assemblies, dumbbell, and CCS polymers. Error margins of ±4% and ±3% were calculated for **P18** and **P19**, respectively. (b) Reduction in d_h of multistar assemblies, dumbbell, and CCS polymers with decreasing pH.

adopting a more coiled conformation, leading to a reduction in d_h values (Figure 8a).

Decreasing the pH below the aggregation pH caused the polymers to aggregate and precipitate from solution due to the insolubility of the uncharged polymers in an acidic medium, which in turn was accompanied by increases in d_h values to 1030 and 770 nm for **P18** and **P19**, respectively. Interestingly, literature values for the aggregation pH of linear PMAA are considerably higher (pH 5.7).[29] The discrepancy in these aggregation pH values highlights the effect of polymer architecture on its physical behavior and can be attributed to the increasingly confined environment of the polymers as mentioned earlier. Accessibility of the charged groups present in the multistar assemblies is a lot more restricted compared to their CCS polymer and linear analogues as a result of their increased segmental density, which is further enhanced by the presence of hydrophobic PMMA TMIs.

The reduction in d_h values of **P18** multistar assemblies, dumbbell, and CCS polymers between pH 11.9 and the aggregation pH (pH 4.1) were 42%, 30%, and 24%, respectively. The latter correlates well with the 22% reduction in d_h observed for CCS polymers **P19** between pH 11.8 and the aggregation pH (pH 5.5). The pH-induced size variation of these polymers clearly demonstrates the PMAA-based multistar assemblies' unique enhanced pH responsiveness. The greater reduction in d_h values of the multistar assemblies and dumbbell polymers can be explained by a cumulative effect; the collapse of multiple CCS polymers within each assembly leads to a more pronounced reduction in d_h than that of a single CCS polymer, as illustrated in Figure 8b. This observation is in agreement with the results obtained by Goh et al. in their studies with PMMA−poly(divinylbenzene) core cross-linked star clusters synthesized via conventional free radical polymerization.[30]

These results demonstrate that as a result of their pH-responsiveness and amphiphilic nature, assemblies such as **P18** have the potential to be employed in a variety of applications such as pH-responsive delivery capsules (encapsulation of payloads that can be released in response to environmental pH changes) and templates for nanostructured materials.

During the reviewing process of this paper, similar work on the synthesis of core cross-linked multistar assemblies connected by degradable disulfide bonds was published with results that corroborate with ours.[31]

Conclusions

Well-defined PMMA, P^{t}BMA, and PMAA-based multistar assemblies have been successfully synthesized and characterized. Issues during the challenging synthesis of these macromolecular architectures such as the increased tendency of the reaction mixture to undergo macrogelation and the difficulty in isolating and characterizing the various polymeric species from the product mixture have been resolved with relevant experimental results from GPC, DLS, and NMR spectroscopy. This facile synthetic method allows these previously inaccessible architectures to be conveniently produced and isolated.

The cleavage of the disulfide-containing TMIs within each polymeric assembly provided evidence for the presence of tristar assemblies and dumbbells in the PMMA-based products consisting of individual star units of $M_w \sim 300$ kDa (PDI ~ 1.17, $d_h \sim 20$ nm), while the P^{t}BMA- and PMAA-based products comprised of higher order tetrastar assemblies, with the P^{t}BMA-based polymers consisting of individual star units of $M_w \sim 600$ kDa (PDI ~ 1.28, $d_h \sim 34$ nm). Images of PMAA-based multistar assemblies in solution obtained via cryo-TEM analysis provided visual proof of the successful synthesis of these unique architectures. It was also determined that these multistar assemblies had an enhanced pH-responsiveness over PMAA CCS polymers, with the d_h of the multistar assemblies and dumbbell polymers varying by 42% and 30%, respectively, compared to 22% for single CCS polymers. This attribute, together with their amphiphilic properties, could be exploited to prepare self-assembling payload delivery vehicles.

Experimental Section

Materials. Methyl methacrylate (MMA, 99%), *tert*-butyl methacrylate (^{t}BMA, >98%), and ethylene glycol dimethacrylate (EGDMA, 98%) were passed over a column of inhibitor remover (top layer) and basic alumina (bottom layer) (Scharlau) twice to remove any inhibitors present. All monomers were stored at 0 °C prior to use. Copper(I) bromide (CuBr, 98%) (Lancaster), copper(I) chloride (CuCl, 97%), 2,2′-dipyridyl (bpy, >99%), benzoyl peroxide (Luperox A75FP) (BPO, 75% (remainder water)), 2-hydroxyethyl disulfide (Tech. Grade), 2-bromoisobutyryl bromide (98%), *tert*-butyl α-bromoisobutyrate (>98%), *p*-toluenesulfonyl chloride (TsCl, >99%), triethylamine (99%) (Ajax Finechem), hydrochloric acid (HCl, 37%) (Merck), sodium hydroxide (NaOH, >99%) (Merck), magnesium sulfate ($MgSO_4$, >99%) (BDH), trifluoroacetic acid (TFA, >98%), chloroform (AR grade), toluene (HPLC grade) (Scharlau), anisole (anhydrous, 99.7%), methanol (GR grade) (Merck), dichloromethane (AR grade), tetrahydrofuran (THF, HPLC grade) (Merck), chloroform-d + 1% v/v tetramethylsilane (TMS) (99.8% deuterated) (Cambridge Isotope Laboratories), dimethyl-d_6 sulfoxide + 1% v/v TMS (99.9% deuterated) (Cambridge Isotope Laboratories), and methanol-d_4 (99.8% deuterated) (Cambridge Isotope Laboratories) were used as received. All reagents were purchased from Sigma-Aldrich unless otherwise specified.

Characterization. Gel permeation chromatography (GPC) of PMMA- and P^{t}BMA-based polymers was carried out on a Shimadzu liquid chromatography system equipped with a Wyatt DAWN EOS MALLS detector (690 nm, 30 mW) and Wyatt OPTILAB DSP interferometric refractometer (690 nm) using Phenomenex Phenogel columns (500, 10^4, and 10^6 Å porosity; 5 μm bead size) operating at 30 °C. THF was used as the eluent at a flow rate of 1 mL/min. Astra software (Wyatt Technology Corp.) was used to determine the weight-average molecular weights (M_ws) using known dn/dc values (dn/dc_{PMMA} = 0.086, dn/dc_{PtBMA} = 0.090)[32] or the injected polymer mass values based on the assumption of 100% mass recovery when the dn/dc values were unknown. GPC of PMAA-based polymers was carried out on a Shimadzu liquid chromatography system equipped with a Wyatt miniDAWN TREOS and Shimadzu RID-10A refractive index detector using Polymer Laboratories mixed columns (3 × PLgel 5 μm MIXED-C) operating at 70 °C. *N*,*N*-Dimethylformamide containing LiBr (0.05 M) was used as the eluent at a flow rate of 1 mL/min. Astra software (Wyatt Technology Corp.) was used to determine the M_ws using injected polymer mass values based on the assumption of 100% mass recovery. Gas chromatography (GC) analysis was performed on a Shimadzu GC-17A gas chromatograph equipped with a DB-5 capillary column (Phenomenex, solid phase 5% phenylsiloxane and 95% dimethylpolysiloxane; 30 m × 0.25 mm × 0.25 μm) and coupled to a GC-MS-QP5000 electron ionization mass spectrometer. Aliquots (0.5 mL) of each reaction mixture were added to methanol (1.5 mL) and mixed thoroughly, and the supernatant was extracted and passed through a 0.45 μm filter. 5 μL of this filtered sample was then injected into the gas chromatograph−mass spectrometer (GC-MS) for analysis. Standard curves of known monomer concentrations were generated and used to determine the concentration of residual monomers after each reaction. Dynamic light scattering (DLS) measurements were performed on a Malvern high-performance particle sizer (HPPS) with a He−Ne laser (633 nm) at an angle of 173° and a temperature of 25 ± 0.1 °C. Freshly prepared 0.1 M NaOH or 0.1 M HCl was used to adjust the pH for DLS experiments involving the PMAA-based polymers. Potentiometric titrations were conducted using a TPS WP81 pH−conductivity−salinity meter. Aqueous polymer solutions (1 mg/mL) were titrated with freshly prepared 0.1 M NaOH, and the activity coefficient ($\alpha = C_b/C_a$, where C_b is the concentration of the added NaOH and C_a is the concentration of methacrylic acid groups) was plotted as a function of pH. ^{1}H and ^{13}C nuclear magnetic resonance (NMR) spectroscopic characterization was carried out on a Varian Unity Plus spectrometer operating at 400 and 100 MHz, respectively. Deuterated chloroform was used as the solvent for PMMA- and P^{t}BMA-based polymer assemblies while deuterated dimethyl sulfoxide was used as the solvent for PMAA-based polymer assemblies. In both cases, the TMS present in deuterated solvents was used as a reference. Deuterated methanol was used as the solvent for PMAA CCS polymers. Cryogenic transmission electron microscopy (cryo-TEM) investigations were undertaken using a Tecnai TF30 transmission electron microscope (FEI Co., Eindhoven, The Netherlands) operated at 200 kV. Images were acquired digitally with a Gatan US1000 2kX2k CCD Camera (Pleasanton, CA).

Synthetic Procedures. *Synthesis of PMMA Telechelic Macroinitiators (TMIs).* Four Schlenk tubes, each charged with MMA (12.0 mL, 112 mmol), B*i*BS (25.9 μL, 90.0 μmol), CuBr (25.8 mg, 180 μmol), and bpy (84.4 mg, 540 μmol), were subjected to three freeze−pump−thaw cycles on a vacuum line (10 Pa). The tubes were then backfilled with argon to restore atmospheric pressure and maintain an inert environment. The Schlenk tubes were subsequently immersed into a preheated oil bath maintained at 100 °C. Individual Schlenk tubes were removed from the oil bath after periods of 1, 2, 3, and 4 h. Immediately after the Schlenk tubes had been removed from the oil bath, they were cooled to room temperature and diluted with THF (10 mL). The reaction mixtures were then passed through columns of basic alumina, and the filtrate was added dropwise to chilled methanol (−18 °C, 120 mL). The resulting precipitates were collected by filtration and dried in vacuo (10 Pa) to yield white powders; 2.36 g (21.0%), 3.09 g (27.5%), 4.63 g (41.2%), and 5.43 g (48.4%). GPC-MALLS: M_w = 59.5 kDa (PDI = 1.13), 68.4 kDa (PDI = 1.15), 79.2 kDa (PDI = 1.13), and 100.2 kDa (PDI = 1.13).

Typical Synthesis of PMMA-Based Core Cross-Linked Dumbbell Polymers and Multistar Assemblies. PMMA MIs (M_w = 11.8 kDa, 1.20 g, 102 μmol), PMMA TMIs (M_w = 59.5 kDa, 0.407 g, 6.78 μmol), bpy (50.8 mg, 325 μmol), EGDMA (0.307 mL, 1.63 mmol), and CuCl (10.7 mg, 108 μmol) were placed in a Schlenk tube, and anisole (10.8 mL) was added. The mixture was subjected to three freeze−pump−thaw cycles on a vacuum line (10 Pa) and then backfilled with argon to restore atmospheric pressure and maintain an inert environment. The Schlenk tube was then immersed into a preheated oil bath maintained at 100 °C for 48 h. After cooling to room temperature, the reaction mixture was diluted with THF (10 mL) and passed through a column of basic alumina. The filtrate was added dropwise to chilled methanol (−18 °C, 100 mL), and the resulting precipitate was collected by filtration and dried in vacuo (10 Pa) to yield **P4** as a white powder, 1.21 g (74.2%). GPC-MALLS: M_w = 488 kDa (PDI = 2.05). Dumbbell polymers and multistar

assemblies were also synthesized using 79.2 and 100.2 kDa PMMA TMIs in an identical fashion, replacing the 59.5 kDa TMIs with molar equivalents of their 79.2 and 100.2 kDa counterparts.

Typical Synthesis of P^{t}BMA-Based Core Cross-Linked Dumbbell Polymers and Multistar Assemblies. P^{t}BMA MIs (M_w = 11.8 kDa, 1.20 g, 102 μmol), PMMA TMIs (M_w = 59.5 kDa, 0.403 g, 6.78 μmol), bpy (50.8 mg, 325 μmol), EGDMA (0.307 mL, 1.63 mmol), and CuCl (10.7 mg, 108 μmol) were placed in a Schlenk tube, and anisole (10.8 mL) was added. The mixture was subjected to three freeze−pump−thaw cycles on a vacuum line and then backfilled with argon to restore atmospheric pressure and maintain an inert environment. The Schlenk tube was then immersed into a preheated oil bath maintained at 100 °C for 48 h. After cooling to room temperature, the reaction mixture was diluted with THF (10 mL) and passed through a column of basic alumina. The filtrate was added dropwise to chilled methanol (−18 °C, 100 mL), and the resulting precipitate was collected by filtration and dried in vacuo (10 Pa) to yield **P14** as a white powder, 0.82 g (51.3%). GPC-MALLS: M_w = 790 kDa (PDI = 1.56). Dumbbell polymers and multistar assemblies were also synthesized using 79.2 and 100.2 kDa PMMA TMIs in an identical fashion, replacing the 59.5 kDa TMIs with molar equivalents of their 79.2 and 100.2 kDa counterparts.

Cleavage of TMIs, Dumbbell Polymers, and Multistar Assemblies. The polymer (1 equiv) was dissolved in THF at a concentration of 0.2 mM (PMMA-based polymers) or 0.05 mM (P^{t}BMA-based polymers) in a Schlenk tube. BPO (100 equiv) was added; the tube was sealed and heated at 60 °C in an oil bath for 48 h. After cooling to room temperature, the reaction mixture was analyzed via GPC.

Synthesis of PMAA-Based Core Cross-Linked Dumbbell Polymers and Multistar Assemblies. The P^{t}BMA-based multistar mixture, **P14** (M_w = 790 kDa, 50.0 mg, 0.063 μmol) synthesized using 59.5 kDa PMMA TMIs was dissolved in dichloromethane (1.5 mL). TFA (0.15 mL, 2.07 mmol) was added, and the mixture was stirred for 24 h. The off-white precipitate that had formed during this time was collected by filtration, washed with acetone (5 mL), and dissolved in methanol (2 mL). This solution was then added dropwise to chloroform (10 mL), and the resulting precipitate was collected by filtration and dried in vacuo (10 Pa) to afford a glassy solid, 23.0 mg (75.9%). GPC-MALLS: 651 kDa (PDI = 1.12).

Acknowledgment. The authors thank Kenneth Goldie for help with cryo-TEM analysis.

Supporting Information Available: Experimental methods for the synthesis of B*i*BS, PMMA, and P^{t}BMA MIs; M_w and PDI vs MMA conversion and kinetic plots of TMI synthesis; GPC RI traces of the chain extension and BPO cleavage of chain-extended **P1**; detailed characterization of the PMMA (**P8**, **P9**, **P11**, **P12**) and P^{t}BMA-based multistar assemblies (**P14**−**16**); calculations determining the effect of MI:TMI ratio on MI and TMI incorporation into the polymer architecture; GPC RI traces and DLS distributions of fractionated polymers **P14a**−**c** before and after cleavage of the disulfide bonds; calculations determining P^{t}BMA MI:PMMA TMI ratio of **P14**; ^{13}C NMR spectra of (a) P^{t}BMA MI, (b) PMMA TMI **P1**, (c) P^{t}BMA-based **P14**, and (d) PMAA-based **P18**; ^{1}H NMR spectra of the acid hydrolysis of **P17**; theoretical M_w calculations for PMAA-based multistar product **P18**; ^{1}H NMR spectra of P^{t}BMA CCS polymer **P17** before and after acid hydrolysis; histogram showing particle size distribution of **P19** by cryo-TEM analysis; activity coefficient (α) against pH plot of PMAA-based multistar product **P18** and CCS polymer **P19**; ^{1}H and ^{13}C NMR spectra of the B*i*BS initiator. This material is available free of charge via the Internet at http://pubs.acs.org.

References and Notes

(1) (a) Wei, H.; Cheng, C.; Chang, C.; Chen, W.-Q.; Cheng, S.-X.; Zhang, X.-Z.; Zhuo, R.-X. *Langmuir* **2008**, *24*, 4564–4570. (b) Zelikin, A. N.; Becker, A. L.; Johnston, A. P. R.; Wark, K. L.; Turatti, F.; Caruso, F. *ACS Nano* **2007**, *1*, 63–69. (c) Zhang, L.; Guo, R.; Yang, M.; Jiang, X.; Liu, B. *Adv. Mater.* **2007**, *19*, 2988–2992. (d) Such, G. K.; Tjipto, E.; Postma, A.; Johnston, A. P. R.; Caruso, F. *Nano Lett.* **2007**, *7*, 1706–1710. (e) Andre, X.; Zhang, M.; Muller, A. H. E. *Macromol. Rapid Commun.* **2005**, *26*, 558–563.

(2) Lee, J.; Kim, H.-J.; Kim, J. *J. Am. Chem. Soc.* **2008**, *130*, 5010–5011.

(3) Sanhai, W. R.; Sakamoto, J. H.; Canady, R.; Ferrari, M. *Nat. Nanotechnol.* **2008**, *3*, 242–244.

(4) (a) Rein, D. H.; Rempp, P.; Lutz, P. J. *Macromol. Chem. Phys.* **1998**, *199*, 569–574. (b) Tsitsilianis, C.; Lutz, P.; Graff, S.; Lamps, J. P.; Rempp, P. *Macromolecules* **1991**, *24*, 5897–5902. (c) Eschwey, H.; Burchard, W. *Polymer* **1975**, *16*, 180–184.

(5) (a) Blencowe, A.; Tan, J. F.; Goh, T. K.; Qiao, G. G. *Polymer* **2009**, *50*, 5–32. (b) Xia, J.; Zhang, X.; Matyjaszewski, K. *Macromolecules* **1999**, *32*, 4482–4484.

(6) Wiltshire, J. T.; Qiao, G. G. *Macromolecules* **2006**, *39*, 4282–4285.

(7) (a) Wiltshire, J. T.; Qiao, G. G. *Aust. J. Chem.* **2007**, *60*, 699–705. (b) Wiltshire, J. T.; Qiao, G. G. *Macromolecules* **2006**, *39*, 9018–9027.

(8) Helms, B.; Guillaudeu, S. J.; Xie, Y.; McMurdo, M.; Hawker, C. J.; Fréchet, J. M. J. *Angew. Chem., Int. Ed.* **2005**, *44*, 6384–6387.

(9) Terashima, T.; Ouchi, M.; Ando, T.; Kamigaito, M.; Sawamoto, M. *Macromolecules* **2007**, *40*, 3581–3588.

(10) (a) Wurm, F.; Nieberle, J.; Frey, H. *Macromolecules* **2008**, *41*, 1909–1911. (b) Wurm, F.; Nieberle, J.; Frey, H. *Macromolecules* **2008**, *41*, 1184–1188. (c) Ge, Z.; Chen, D.; Zhang, J.; Rao, J.; Yin, J.; Wang, D.; Wan, X.; Shi, W.; Liu, S. *J. Polym. Sci., Part A: Polym. Chem.* **2007**, *45*, 1432–1445. (d) Nguyen, P. M.; Hammond, P. T. *Langmuir* **2006**, *22*, 7825–7832. (e) Barriau, E.; Marcos, A. G.; Kautz, H.; Frey, H. *Macromol. Rapid Commun.* **2005**, *26*, 862–867. (f) Namazi, H.; Adeli, M. *Polymer* **2005**, *46*, 10788–10799. (g) An, S. G.; Cho, C. G. *Polym. Bull.* **2004**, *51*, 255–262. (h) Gitsov, I.; Lambrych, K. R.; Remnant, V. A.; Pracitto, R. *J. Polym. Sci., Part A: Polym. Chem.* **2000**, *38*, 2711–2727. (i) Iatrou, H.; Willner, L.; Hadjichristidis, N.; Halperin, A.; Richter, D. *Macromolecules* **1996**, *29*, 581–591. (j) Njikang, G. N.; Cao, L.; Gauthier, M. *Macromol. Chem. Phys.* **2008**, *209*, 907–918. (k) Njikang, G. N.; Cao, L.; Gauthier, M. *Langmuir* **2008**, *24*, 12919–12927. (l) Gitsov, I.; Hamzik, J.; Ryan, J.; Simonyan, A.; Nakas, J. P.; Omori, S.; Krastanov, A.; Cohen, T.; Tanenbaum, S. W. *Biomacromolecules* **2008**, *9*, 804–811. (m) Simonyan, A.; Gitsov, I. *Langmuir* **2008**, *24*, 11431–11441.

(11) (a) Gitsov, I. *J. Polym. Sci., Part A: Polym. Chem.* **2008**, *46*, 5295–5314. (b) Gitsov, I.; Simonyan, A.; Vladimirov, N. G. *J. Polym. Sci., Part A: Polym. Chem.* **2007**, *45*, 5136–5148. (c) Lambrych, K. R.; Gitsov, I. *Macromolecules* **2003**, *36*, 1068–1074. (d) Emrick, T.; Hayes, W.; Fréchet, J. M. J. *J. Polym. Sci., Part A: Polym. Chem.* **1999**, *37*, 3748–3755. (e) Matyjaszewski, K.; Shigemoto, T.; Frechet, J. M. J.; Leduc, M. *Macromolecules* **1996**, *29*, 4167–4171. (f) Gitsov, I.; Wooley, K. L.; Frechet, J. M. J. *Angew. Chem., Int. Ed.* **1992**, *31*, 1200–1202.

(12) Lee, E.; Jeong, Y.-H.; Kim, J.-K.; Lee, M. *Macromolecules* **2007**, *40*, 8355–8360.

(13) (a) Connal, L. A.; Li, Q.; Quinn, J. F.; Tjipto, E.; Caruso, F.; Qiao, G. G. *Macromolecules* **2008**, *41*, 2620–2626. (b) Furukawa, T.; Ishizu, K. *Macromolecules* **2005**, *38*, 2911–2917.

(14) Furukawa, T.; Uchida, S.; Ishizu, K. *J. Appl. Polym. Sci.* **2007**, *105*, 1543–1550.

(15) Johnson, J. A.; Baskin, J. M.; Bertozzi, C. R.; Koberstein, J. T.; Turro, N. J. *Chem. Commun.* **2008**, *26*, 3064–3066.

(16) Oral, E.; Peppas, N. A. *J. Biomed. Mater. Res., Part A* **2004**, *68A*, 439–447.

(17) Johnson, J. A.; Lewis, D. R.; Diaz, D. D.; Finn, M. G.; Koberstein, J. T.; Turro, N. J. *J. Am. Chem. Soc.* **2006**, *128*, 6564–6565.

(18) Li, Y.; Armes, S. P. *Macromolecules* **2005**, *38*, 8155–8162.

(19) Initial attempts to cleave the disulfide bond using more conventional reagents, such as dithiothreitol (DTT) and tri-*n*-butylphosphine (^{n}Bu$_3$P), were only partially successful, resulting in incomplete cleavage as determined by the presence of bimodal peaks in the GPC RI traces.

(20) The low PDI values of the polymers relative to the apparent broadness of the GPC RI traces are due to limitations of the

GPC-MALLS system which uses light scattering data to calculate the M_w and PDI. This technique is generally considered to be very accurate, but unfortunately the high molecular weight of the star polymers being analyzed generates a very intense light scattering (LS) signal which can mask the LS signal of lower molecular weight polymers and hence underestimate the PDI.

(21) A 15:1 MI:TMI ratio indicates that 1 mol of TMI is added for every 15 mol of MIs used in the synthesis of the core cross-linked assemblies. 25:1 and 35:1 ratios indicate the respective reduction in the amount of TMIs used.

(22) A possible explanation for the slight increase in M_w (113 to 119 kDa) of polymer fraction **P12c** (prepared using TMI **P3** at a MI:TMI = 35) after attempted cleavage is the polymerization of accessible pendent double bonds present on partially formed stars or low molecular weight material initiated by radicals generated by BPO.

(23) Arm number calculation based on a core fraction of 0.2 (derived from the complete conversion of EGDMA determined via GC-MS).

(24) He, T.; Adams, D. J.; Butler, M. F.; Yeoh, C. T.; Cooper, A. I.; Rannard, S. P. *Angew. Chem., Int. Ed.* **2007**, *46*, 9243–9247.

(25) Gurr, P. A.; Qiao, G. G.; Solomon, D. H.; Harton, S. E.; Spontak, R. J. *Macromolecules* **2003**, *36*, 5650–5654.

(26) Muthukrishnan, S.; Plamper, F.; Mori, H.; Muller, A. H. E. *Macromolecules* **2005**, *38*, 10631–10642.

(27) The dense edges of the cryo-TEM images are a result of the underfocus (ca. 2 μm) used to improve the phase contrast of the polymers. The expected decreasing density profile of the star polymer from the core of the macromolecule was not observed due to the phase contrast between the core and the corona being insufficient for observation of such a density variation.

(28) Plamper, F. A.; Becker, H.; Lanzendoerfer, M.; Patel, M.; Wittemann, A.; Ballauff, M.; Muller, A. H. E. *Macromol. Chem. Phys.* **2005**, *206*, 1813–1825.

(29) Ruiz-Perez, L.; Pryke, A.; Sommer, M.; Battaglia, G.; Soutar, I.; Swanson, L.; Geoghegan, M. *Macromolecules* **2008**, *41*, 2203–2211.

(30) Goh, T. K.; Sulistio, A. P.; Blencowe, A.; Johnson, J. W.; Qiao, G. G. *Macromolecules* **2007**, *40*, 7819–7826.

(31) He, T.; Adams, D. J.; Butler, M. F.; Cooper, A. I.; Rannard, S. P. *J. Am. Chem. Soc.* **2009**, *131*, 1495–1501.

(32) *Polymer Handbook*, 4th ed.; Brandrup, J., Immergut, E. H., Eds.; Wiley-Interscience: Chichester, 1998.